Some novel concepts in multipyramid wavefront sensing

Emiliano Diolaiti[*a], Andrea Tozzi[b], Roberto Ragazzoni[b,c], Debora Ferruzzi[b],
Elise Vernet-Viard[b], Simone Esposito[b], Jacopo Farinato[b], Armando Riccardi[b]
[a]Università di Padova – Dipartimento di Astronomia; [b]Osservatorio Astrofisico di Arcetri;
[c]Max Planck Institut für Astronomie (as W. Paul awardee by the Alexander von Humboldt Society)

ABSTRACT

We describe some novel technical approaches to implement multi-pyramid wavefront sensing, partially extendable to single pyramid and to any MCAO system. First we introduce an achromatic version of the pyramid, which allows for a much better spatial resolution on the pupil and also relaxes the specifications in term of turned edges. Then we discuss the effect of pupil distortion occurring in the layers above the ground during the open loop phases of a MCAO system. The distribution of tolerances in a layer-oriented AO system makes attractive, at least in some cases, the usage of pairs of lenslet arrays, leaving only the pyramids free to move over the Field of View, hence relaxing the requirements in terms of roll and yaw in their positioning. Finally we discuss a possible usage of the Modulation Transfer Function as a valuable tool to estimate the correction of a certain Zernike polynomial, achievable with a pyramid wavefront sensor. These items are sketched along with a status of their practical implementation and possible future extensions.

Keywords: Pyramid Wavefront Sensor, Achromatic Pyramid, MCAO, Layer-Oriented, pupil re-imaging, MTF

1. INTRODUCTION

The Pyramid Sensor[1] (PS), proposed a few years ago as an alternative wavefront sensor (WFS) for astronomical applications, has been implemented so far on AdOpt@TNG[2] and it has been extensively tested in the laboratory[3]. After several engineering runs at the Telescopio Nazionale Galileo (TNG), the AdOpt@TNG module is now fully operating[4]. Some new instruments, currently in their design phase, will be equipped with a PS, used both in the single-reference Adaptive Optics (AO) mode[5,6] and in the Multi-Conjugate Adaptive Optics mode[7,8]. Several new ideas have been recently proposed to improve the performance of the PS and a considerable theoretical work has been carried out to better understand its properties. We just mention here the diffusing plate concept[9], as a way to accomplish the pyramid modulation without any moving part, and the more recent idea that in a real system the residual turbulence at the wavefront sensing wavelength might be fully equivalent to a dynamic modulation of the pyramid, hence no additional vibration would be necessary to operate the sensor[10]. Also on a more technical ground several concepts have been worked out, in most cases to overcome a practical limit or constraint. Some of these achievements, either technical or theoretical, are reported in this paper.

2. ACHROMATIC PYRAMID

A pyramid prism, placed at the focal plane of the telescope, splits the image of the reference star into four beams, which are then focused by a lens in four pupil images. Of course these re-imaged pupils must fulfill some dimensional requirements, concerning both the diameter of each single pupil and their reciprocal distance, in order to fit the area of

[*] diolaiti@pd.astro.it; phone +39 049 8293494; fax 049 8759840; http://www.pd.astro.it; Università di Padova – Dipartimento di Astronomia; vicolo dell'Osservatorio 2; I-35122 Padova; Italy

the detector used for wavefront sensing. According to Figure 1 (left), the angular separation of the beams formed by the pyramid is

$$\beta = (n-1)\alpha \tag{1}$$

where n is the refractive index of the glass. Tipically the beam separation β is a few times the angular size of each beam, given by $\theta = 1/F$, where F is the focal ratio. Adopting typical values of the focal ratio, one can easily deduce that the vertex angle of the pyramid is in the range α = 1-2°.

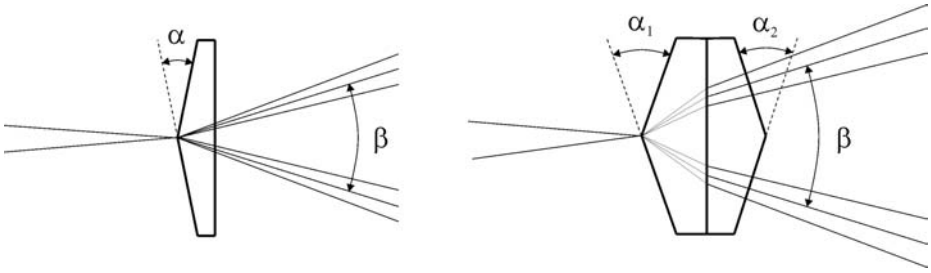

Figure 1. Pyramid angles definition.

The most important practical drawback of such a small vertex angles is represented by the practical difficulties in the manufacturing of the prisms, so far accomplished by mechanical grinding of crown glasses. Polishing tests have shown that the best edge sharpness achieved up to now is about 10μm, which is not much smaller than the typical PSF size at the focal plane of a modern telescope. Considering a F/45 focal plane and a wavefront sensing wavelength λ = 0.7μm, the diffraction-limited PSF has a FWHM of about 30μm, just 3 times larger than the currently achieved edge quality; it is easy to see by numerical simulations that this translates into an energy loss of approximately 50% in diffraction limited conditions. At the moment conventional pyramid manufacturing is investigated to achieve edges of about 5μm. Even though alternative techniques for pyramid manufacturing are under test[11], a valid solution to the problem is the use of double pyramids (Figure 1, right). In fact the beam divergence introduced by a double pyramid prism is proportional to the difference of the two vertex angles

$$\beta = (n-1)(\alpha_1 - \alpha_2) \tag{2}$$

hence it is possible to adopt much larger vertex angles for the individual prisms, while keeping the beam divergence β fixed. This makes the grinding process easier and ensures sharper edges. In this respect, the optimal vertex angle is around 30°. It should be stressed than only the edge quality of the first pyramid is important; as it is evident from Figure 1 (right), only the central part of the faces of the second prism are actually illuminated by the beams refracted by the first prism. A double pyramid is characterized by a maximum acceptance angle, beyond which the ray refracted by the first prism hits the wrong face of the second pyramid. Furthermore, since the total thickness of the two prisms is obviously larger than a single pyramid, due also to the larger vertex angles, a double pyramid might introduce considerable chromatic effects in the refracted beams. On the other hand, it is possible to use different glasses for the two prisms to compensate the chromatic aberration. This solution has been adopted to design the achromatic pyramids for AGW, the first light AO module for LBT[5].

The design has been carried on in two steps. First of all the vertex angle of the second pyramid and the two glasses have been selected in order to minimize the chromatic effect, with a constraint on the inter-distance among the four pupil images, imposed by the detector geometry. The vertex angle of the first prism has been fixed to α_1 = 30°. This preliminary optimization has been performed by an extensive search of the parameter space, using an IDL program. The initial design has been finely tuned by a ray-tracing program (ZEMAX-EE v.10), optimizing a similar figure of merit and adopting as free variables for the optimization the vertex angle of the second pyramid and the thickness of the two prisms. A preliminary design of the double pyramid for AGW, obtained with this method, is shown in Figure 2.

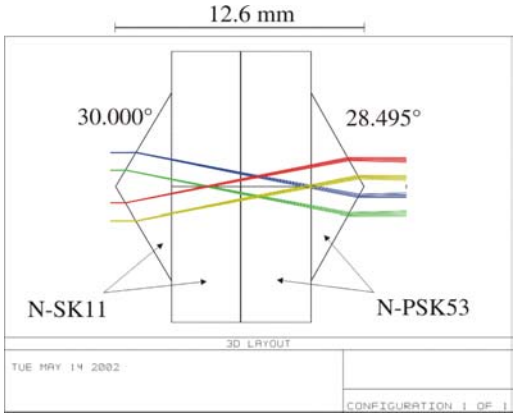

Figure 2. Preliminary optical and mechanical design of the achromatic pyramid for AGW.

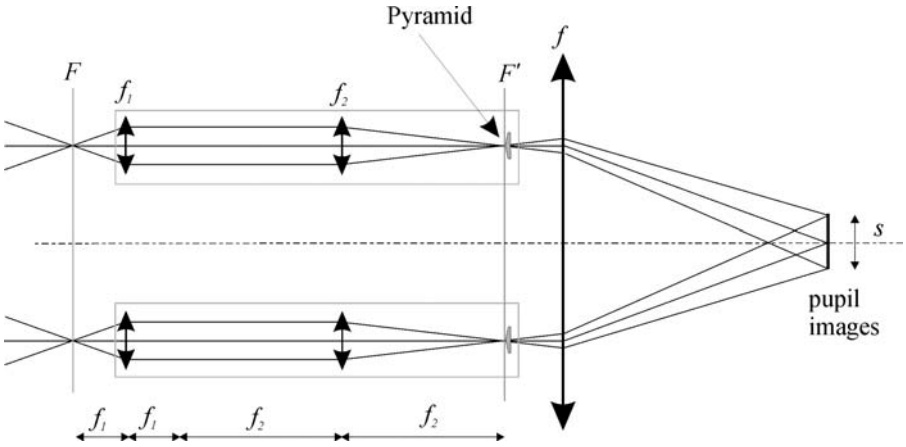

Figure 3. Conceptual optical design of the Layer-Oriented WFS aboard VLT. The two lenses of focal length f_1 and f_2 and the pyramid are held together by a common mechanical support. Only one pupil image out of four is shown here for simplicity.

3. LENSLET ARRAYS IN A PYRAMID-BASED WFS?

A straightforward application of the PS is related to the layer-oriented approach12, an implementation of the Multi-Conjugated Adaptive Optics (MCAO) concept13. In this multi-reference mode, each star is associated to a pyramid and the pupil images formed by the various prisms placed in the focal plane are combined by a single re-imaging optics, in a way that the signals of the stars are optically co-added, improving the signal-to-noise ratio wherever at least two star footprints overlap. A known problem of the layer-oriented approach is the size of the re-imaged pupils, which imposes the use of large detectors with massive binning. This trouble may be overcome14 enlarging the focal ratio of each star individually rather than collectively. In this way the pupil size, which is inversely proportional to the focal ratio, can be arbitrarily shrinked, while the inter-distance between the various stars across the covered Field of View (FoV) is retained unchanged. The basic principle is shown in Figure 3. The focal plane before the WFS is indicated by the vertical gray line. The rays are arriving from a certain FoV in telecentric mode at a focal ratio F. The beam of each reference star is collimated by a lens of focal length f1, producing a small pupil image for each sensed star. A second lens of focal length f2, placed a distance f2 to the right of the intermediate pupil (hence the exit pupil remains at infinity), forms an enlarged image of the reference star with an equivalent focal ratio $F' = kF$, where we define the

shrinking factor $k = f_2/f_1$. A pyramid placed in this position splits the light in four beams, which are focused by the objective of focal length f in four pupil images. The re-imaged pupils corresponding to different reference stars are collected by the objective, which optically co-adds the light of the stars. The size of the each pupil image is

$$s = \frac{1}{kF} \tag{3}$$

This approach is being implemented in the layer-oriented channel of the WFS for MAD, the ESO MCAO demonstrator[15]. The two lenses and the pyramid associated to each star are mechanically held together into a single structure, hereafter called *star enlarger* which might be moved perpendicularly to the input focal plane by two independent linear movements. If the structure is tilted by a certain angle, the exit pupil is substantially displaced by the same angle. A tolerance on this tilt is derived by imposing that the pupil displacement is much smaller than the sampling sub-aperture. In fact, in the single-reference mode a pupil shift does not represent a particular problem, whereas in the multi-reference mode differential shifts among the various pupil images translate into a smearing and a loss of information on the wavefront to be reconstructed. Imposing that the pupil shift is 1/10 of the sub-aperture size and assuming a $N \times N$ sampling of the pupil, one obtains a tolerance on the above mentioned tilt angle of

$$\sigma_\theta = \frac{1}{10 \times NkF} \tag{4}$$

In the case of MAD, we have $N = 8$, $F = 20$ and $k = 15$, obtaining $\sigma_\theta \approx 10''$, a quite tight constraint.

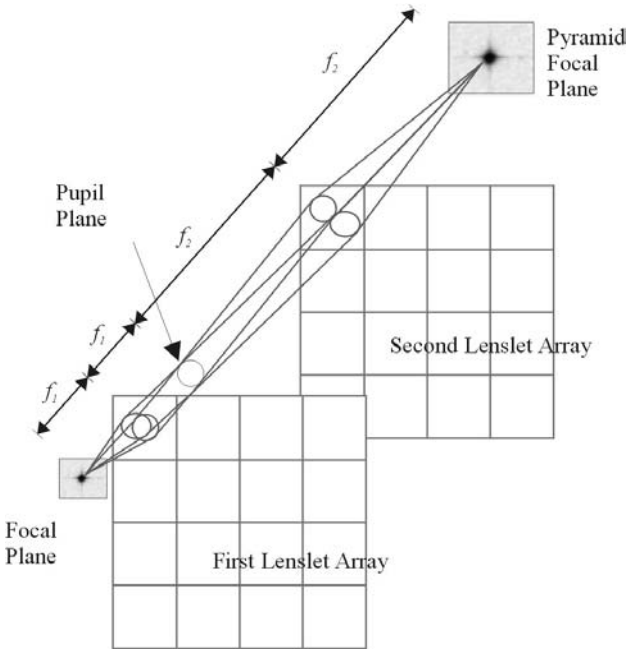

Figure 4. The lenses of focal length f_1 and f_2 illustrated in Figure 3 are replaced by two lenslet arrays. The star image in the pyramid focal plane is enlarged by the two lenslet arrays by a factor k.

This alignment tolerance may be considerably relaxed if all the lenses of focal length f_1 and f_2 are replaced by two lenslet arrays, with the same pitch but focal lengths f_1 and f_2 respectively (Figure 4). In this case the two lenslet arrays, once aligned and assuming negligible misalignment errors among the various lenslets, do not introduce any differential tilt among the exit pupils corresponding to different reference stars. Only the pyramids have to be moved to pick the

light of the reference stars. It should be stressed that the misalignment of the various pyramids is not critical, at least to first order, since it does not introduce any pupil shift. It might be desirable to let the two lenslet arrays move, either rotate about the optical axis or translate perpendicularly to it, in order to maximize the focal plane coverage. Of course these movements would be accomplished by rotating or translating the two arrays together, as a unique rigid body, thus preventing any additional misalignment source.

The major drawback of the lenslet arrays solution is represented by the FoV coverage. In the solution presented in Figure 3, in fact, the first star enlarger placed in position can effectively cover the whole FoV. The second star enlarger might cover the whole FoV except a small region, represented by the area covered by the first star enlarger multiplied by the shrinking factor k. In the lenslet arrays solution, instead, the first pyramid is positioned in order to pick one star. The useful area is not the whole focal plane, because the second lenslet array, projected on the sky, covers an area k^2 smaller than the first one. We might define a filling factor proportional to $1/k^2$. Hence the first pyramid may pick up the light of the stars falling on a region of the sky which is at most $1/k^2$ times the whole FoV. The second pyramid has basically the same filling factor, minus the area occupied by the first pyramid and so on. Given the dependence of the filling factor on k, it is clear that the lenslet arrays solution might be implemented only for moderate shrinking factors. This situation is typical, for instance, of AO applications in the visible, where the coherence length r_0 of the atmosphere[16] is smaller than in the infrared; in order to have a proper sampling of the pupil, it is therefore necessary to increase the pupil size, because the linear pixel size cannot be made arbitrarily small. An increase in the pupil size translates into a decrease of the shrinking factor k, according to Equation (3). With a shrinking factor comparable to unit, e.g. $k \approx 2$, the focal plane filling factor is not so small and it might be worthwhile to consider the lenslet arrays solution.

4. PUPIL DISTORTION IN LAYER-ORIENTED MCAO

In principle there is no any limit on the pupil shrinking factor k, defined in the previous Section. While this statement strictly holds when the ground layer is considered, an upper limit does exist if one considers the re-imaging errors of the high-altitude portions of the turbulence[14]. The layer-oriented system forms an anamorphic copy of the atmosphere and the detector which measures the high altitude turbulence is placed in a certain plane, conjugated for instance with the strongest high altitude layer. The concept of conjugated plane, however, is related to a nominal situation in which the aberrations are small. When this condition is not true, as in open loop and in the bootstrap phase, the layer appears distorted on the detector plane. This effect is more considerable in the solution presented in the previous Section, either with the star enlargers or the two lenslet arrays. A consequence of the shrinking factor k, in fact, is that the considered conjugated plane is formed at a distance from the re-imaged pupil k times larger than in an equivalent approach yielding the same pupil size but with no star enlargers or lenslet arrays (see Figure 5, left). A nominal and an aberrated ray intersecting at the same point of the telescope pupil (Figure 5, right) are laterally displaced on the high altitude layer; following the previous reasoning, this displacement is approximately k times larger in the approach based on the star enlargers. According to Figure 5 (right), the intersection of the aberrated ray with the high altitude layer may be approximated to the first order with the back-projection of the ray itself, seen from the entrance pupil. This projection depends only on the arrival angle $\alpha(0)$ at the ground. At a given altitude h, the linear distance between the nominal ray and the projected one in the approach with no pupil shrinking is

$$\Delta l_{proj} = h\alpha(0) \tag{5}$$

and becomes k times larger with the star enlargers. Assuming $\alpha(0) \approx \lambda/r_0$, one obtains

$$\Delta l_{proj} \approx k\frac{\lambda}{r_0}h \tag{6}$$

This re-imaging error is negligible if it is smaller than the coherence length $r_0(h)$ at the layer altitude. Considering that the r_0 of the upper part of the atmosphere is usually 2-3 times larger than the overall value and assuming typical r_0

values for the Cerro Paranal atmosphere[17], one obtains that the pupil shrinking factor must be $k \leq 80, 28, 10$ for respectively excellent, good and median seeing conditions.

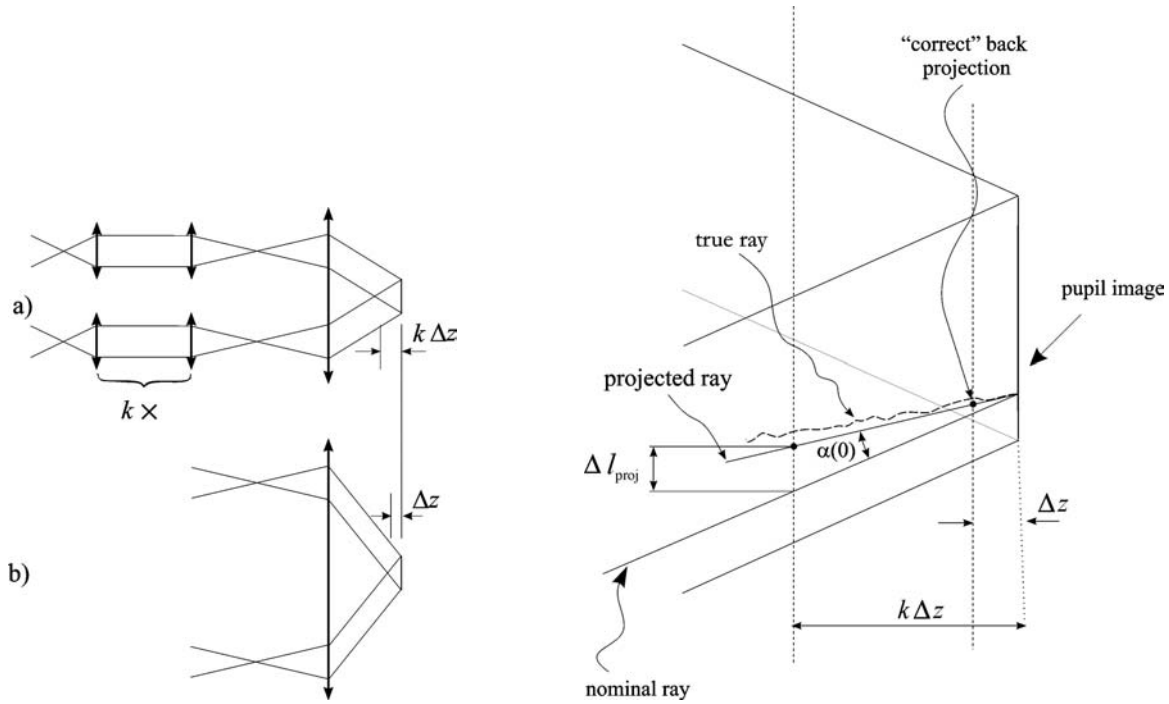

Figure 5. Left: re-imaging a high-altitude layer in the *star enlargers* approach described in Sec. 3. We just mention here that the equivalent configuration shown in (b), giving the same pupil size as (a) but with no star enlarger, might not be feasible, because it might require an exceedingly fast focal ratio of the re-imaging optics. Right: zoom of the anamorphic copy of the atmosphere formed by the layer-oriented system.

5. ASSESSING THE PUPIL RE-IMAGING QUALITY BY THE MTF

Both pupil-plane and Shack-Hartmann WFSs require a re-imaging of the pupil somewhere. In the Shack-Hartmann WFS the re-imaging of the pupil is necessary to create a pupil plane where to place the lenslet array. The issue of the imaging quality is in a certain sense common to all these WFSs. In general the faster is the pupil re-imager, the more difficult is to obtain a good quality of the image. As we have shown in Sec. 3, in a layer-oriented system it might be necessary to use fast re-imaging optics to reduce the pupil size and fit it to a small detector. The same constraint exists in modern Shack-Hartmann WFSs, which usually adopt small lenslet arrays directly glued to the detector.

A suitable method to assess the quality of the pupil image relies on the Modulation Transfer Function (MTF) of the re-imaging lens. The MTF represents the hampering factor of a certain spatial frequency in the observed scene. In a WFS the scene is represented by the pupil and its aberrations, which are usually expressed in term of Zernike polynomials. Each polynomial might be associated to a particular spatial frequency, inversely proportional to the number of radial or azimuthal zeroes. High-order polynomials are seen with a smaller gain than low-order ones (Figure 6). The maximum spatial frequency of interest at which the MTF should be evaluated is inversely proportional to the sub-aperture size, i.e.

$$u_c = \frac{NF}{f}, \tag{7}$$

where N is the number of sub-apertures across one pupil diameter, f is the focal length of the pupil re-imager and F is the focal ratio of the beams collected by the lens. The pupil re-imager designed for the layer-oriented WFS for MAD-VLT[15] is illustrated in Figure 7. In this case the relevant quantities are $N = 8$, $f = 115.7$mm and $F = 300$, corresponding to a maximum frequency $u_c \approx 21$ cycles/mm. As it may be seen, the re-imaging quality is very close to the diffraction limit.

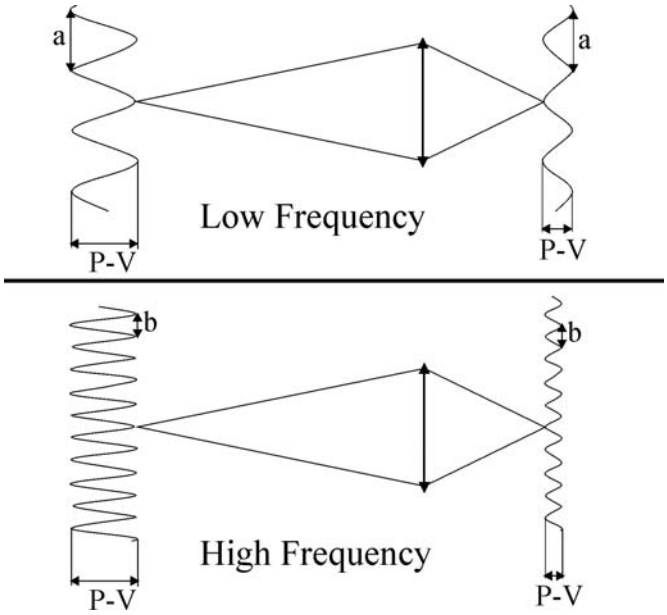

Figure 6. Pupil re-imaging errors: the Peak-to-Valley (P-V) of a given wavefront pattern is differently hampered depending on its spatial frequency. High-spatial frequency aberrations are imaged with a smaller gain than low-frequency patterns.

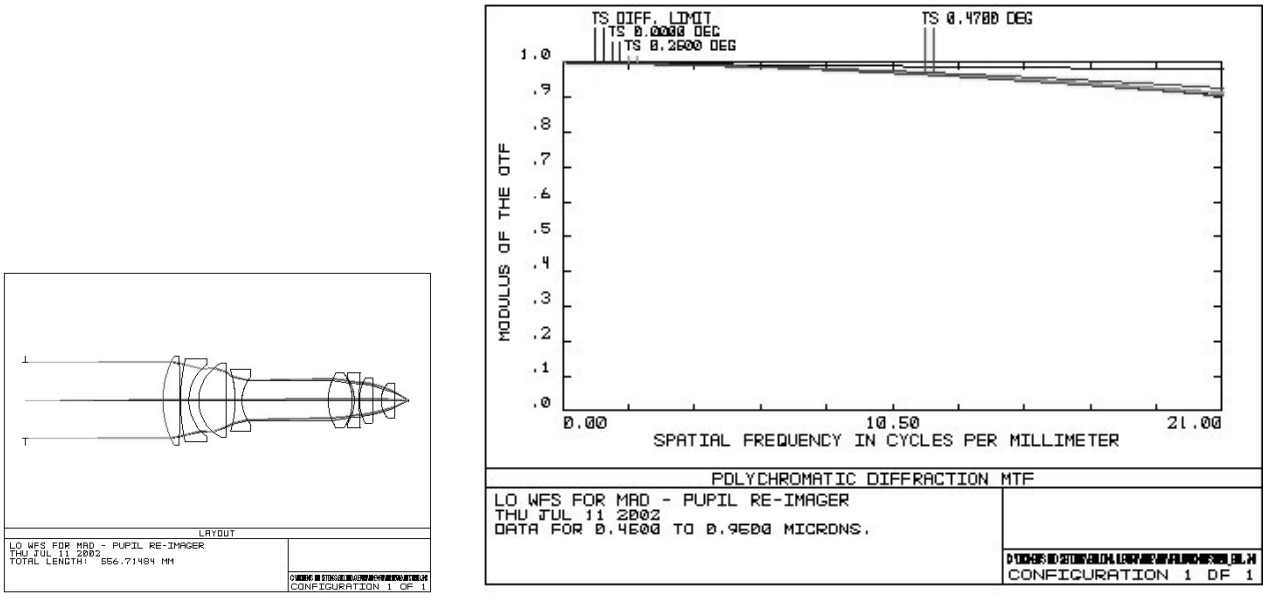

Figure 7. Left: optical layout of the F/1 pupil re-imager in the Layer-Oriented WFS for MAD-VLT. Right: MTF of pupil-reimager; the highest curve in the plot is the diffraction MTF.

REFERENCES

1. R. Ragazzoni, "Pupil plane wavefront sensing with an oscillating prism", *J. Mod. Opt.* **43**, pp. 289-293, 1996.
2. R. Ragazzoni, A. Baruffolo, J. Farinato, A. Ghedina, E. Marchetti, S. Esposito, L. Fini, P. Ranfagni, F. Bortoletto, M. D'Alessandro, M. Ghigo, G. Crimi, "Final commissioning phase of the AdOpt@TNG module", SPIE **4007**, pp. 57-62, 2000.
3. S. Esposito, O. Feeney, A. Riccardi, "Laboratory test of a pyramid wavefront sensor", SPIE **4007**, pp. 416-422, 2000.
4. A. Ghedina, M. Cecconi, R. Ragazzoni R., J. Farinato, A. Baruffolo, G. Crimi, E. Diolaiti, S. Esposito, L. Fini, M. Ghigo, E. Marchetti, T. Niero, A. Puglisi, "Testing the Pyramid Wavefront sensor on the sky", *this Conference*.
5. S. Esposito, A. Riccardi, J. Storm, M. Accardo, C. Baffa, R. Biasi, V. Biliotti, G. Brusa, M. Carbillet, D. Ferruzzi, L. Fini, I. Foppiani, D. Gallieni, A. Puglisi, R. Ragazzoni, P. Ranfagni, P. Salinari, W. Seifert, P. Stefanini, A. Tozzi, C. Verinaud, "First light AO system for LBT", *this Conference*.
6. J. Costa, S. Hippler, M. Feldt, S. Esposito, R. Ragazzoni, P. Bizenberger, J. Baehr, T.F. Henning, "PYRAMIR: a near-infrared pyramid wavefront sensor for the Calar Alto adaptive optics system", *this Conference*.
7. E. Marchetti, N.N. Hubin, E. Fedrigo, R. Donaldson, R. Conan, M. Le Louarn, B. Delabre, F. Franza, D. Baade, C. Cavadore, A. Balestra, J.-L. Lizon, R. Ragazzoni, J. Farinato, E. Vernet-Viard, E. Diolaiti, D.J. Butler, S. Hippler, A. Amorin, "MAD: the ESO multiconjugate adaptive optics demonstrator", *this Conference*.
8. R. Ragazzoni, T. Herbst, D. Andersen, P. Bizenberg, H.W. Rix, R-R. Rohloff, C. Arcidiacono, E. Diolaiti, S. Esposito, J. Farinato, A. Riccardi, E. Vernet-Viard, P. Salinari, "NIRVANA: a visible MCAO channel for LBT", *this Conference*.
9. R. Ragazzoni, E. Diolaiti, E. Vernet, "A pyramid wavefront sensor with no dynamic modulation", *Opt. Comm.* **208**, pp. 51-60, 2002.
10. J. Costa, R. Ragazzoni, S. Hippler, A. Ghedina, J. Farinato, "Is there need of any modulation in the pyramid wavefront sensor?", *this Conference*.
11. M. Ghigo, F. Perennes, R. Ragazzoni, "Manufacturing by deep x-ray lithography of pyramid wavefront sensors for astronomical adaptive optics", *this Conference*.
12. R. Ragazzoni, J. Farinato, E. Marchetti, "Adaptive optics for 100-m-class telescopes: new challenges require new solutions", *SPIE* **4007**, pp. 1076-1087, 2000.
13. J.-M. Beckers, "Detailed compensation of atmospheric seeing using multiconjugate adaptive optics", *SPIE* **1114**, p. 215, 1989.
14. R. Ragazzoni, E. Diolaiti, E. Vernet, J. Farinato, E. Marchetti, "Arbitrarly small pupils in layer-oriented multi-conjugate adaptive optics", *in preparation*.
15. E. Vernet-Viard, R. Ragazzoni, E. Diolaiti, R. Falomo, J. Farinato, E. Fedrigo, E. Marchetti, C. Arcidiacono, A. Baruffolo, S. Esposito, M. Tordi, M. Carbillet, C. Verinaud, "The Layer Oriented wavefront sensor for MAD: status and progress report", *this Conference*.
16. D.L. Fried, "Statistics of a Geometric Representation of Wavefront Distortion", *J. Opt. Soc. Am.* **55**, pp. 1427-1435, 1965.
17. M. Le Louarn, N. Hubin, M. Sarazin, A. Tokovinin, "New challenges for adaptive optics: extremely large telescopes", *MNRAS* **317**, pp. 535-544, 2000.